Hindawi
Advances in Materials Science and Engineering
Volume 2023, Article ID 9802670, 1 page
https://doi.org/10.1155/2023/9802670

Retraction

Retracted: Optimization of Water Absorption and Mechanical and Thermal Behavior of Polylactic Acid/Chitosan/Titanium Carbide

Advances in Materials Science and Engineering

Received 11 July 2023; Accepted 11 July 2023; Published 12 July 2023

This article has been retracted by Hindawi following an investigation undertaken by the publisher [1]. This investigation has uncovered evidence of one or more of the following indicators of systematic manipulation of the publication process:

(1) Discrepancies in scope
(2) Discrepancies in the description of the research reported
(3) Discrepancies between the availability of data and the research described
(4) Inappropriate citations
(5) Incoherent, meaningless and/or irrelevant content included in the article
(6) Peer-review manipulation

The presence of these indicators undermines our confidence in the integrity of the article's content and we cannot, therefore, vouch for its reliability. Please note that this notice is intended solely to alert readers that the content of this article is unreliable. We have not investigated whether authors were aware of or involved in the systematic manipulation of the publication process.

Wiley and Hindawi regrets that the usual quality checks did not identify these issues before publication and have since put additional measures in place to safeguard research integrity.

We wish to credit our own Research Integrity and Research Publishing teams and anonymous and named external researchers and research integrity experts for contributing to this investigation.

The corresponding author, as the representative of all authors, has been given the opportunity to register their agreement or disagreement to this retraction. We have kept a record of any response received.

References

[1] S. Krishnamohan, H. Anandaram, V. Rathinam et al., "Optimization of Water Absorption and Mechanical and Thermal Behavior of Polylactic Acid/Chitosan/Titanium Carbide," *Advances in Materials Science and Engineering*, vol. 2022, Article ID 5176584, 8 pages, 2022.

Hindawi
Advances in Materials Science and Engineering
Volume 2022, Article ID 5176584, 8 pages
https://doi.org/10.1155/2022/5176584

Research Article

Optimization of Water Absorption and Mechanical and Thermal Behavior of Polylactic Acid/Chitosan/Titanium Carbide

S. Krishnamohan,[1] **Harishchander Anandaram**,[2] **V. Rathinam**,[3] **S. Kaliappan**,[4] **S. Sekar**,[5] **Pravin P Patil**,[6] **Asheesh Kumar**,[7] **and Venkatesan Govindaraajan**[8]

[1]*Department of Mechanical Engineering, E.G.S. Pillay Engineering College, Nagapattinam, Tamil Nadu, India*
[2]*Centre for Computational Engineering and Networking (CEN), Amrita Vishwa Vidyapeetham, Coimbatore, Tamil Nadu, India*
[3]*Automobile Engineering Department, VNR Vignana Jyothi Institute of Engineering and Technology, Hyderabad, Telangana, India*
[4]*Department of Mechanical Engineering, Velammal Institute of Technology, Chennai, Tamil Nadu, India*
[5]*Department of Mechanical Engineering, Rajalakshmi Engineering College, Rajalakshmi Nagar, Thandalam, Chennai, India*
[6]*Department of Mechanical Engineering, Graphic Era Deemed to Be University, Bell Road, Clement Town, Dehradun, Uttarakhand, India*
[7]*Mechanical Engineering Department, Mahatma Gandhi Institute of Technology, Hyderabad, Telangana, India*
[8]*Department of Mechanical Engineering, Haramaya Institute of Technology, Haramaya University, Dire Dawa, Ethiopia*

Correspondence should be addressed to Venkatesan Govindaraajan; venkatesanggg2011@gmail.com

Received 3 April 2022; Revised 14 July 2022; Accepted 25 July 2022; Published 8 October 2022

Academic Editor: Penchal Reddy

Nanocomposites are being studied for their mechanical, thermal, and water absorption capabilities. Polylactic acid/chitosan blends have been studied extensively for their physical, mechanical, and morphological properties. Although the three materials have been blended, no research has been done on the mechanical or morphological properties of PLA/CS/TiC NPs. PLA/CS bonding is quite deprived, and thus researchers are trying to improve it by introducing TiC NPs; this would improve the composites' overall quality (mechanical and thermal characteristics as well as water absorption) by increasing the strength of the bind between the two materials. The impacts of TiC NPs on PLA/CS properties are studied using FTIR and XRD and thermal (TGA) and mechanical investigations. Titanium carbide nanoparticles in the polylactic acid/chitosan matrix increase the mechanical characteristics of the materials. As an outcome, the TiC content in the sample rises to 4 wt % even though adding TiC NPs increased the mechanical properties by up to 2%. The findings of this study might be applied to the development of environmentally friendly casings.

1. Introduction

Renewable bio-sourced components have become more popular in recent years as a replacement for petroleum-based goods [1]. To put it another way, a biomaterial is anything that may be utilized for a long length of time to cure, enhance, or replace an organ or tissue in the body [2, 3]. A number of advantages of bio-composite materials include the capacity for scientists and engineers to alter the qualities of the material. Chitosan (CS) is a bio-based polymer that has no genuine petrochemical equivalent since its inherent qualities are so unique and important. Thus, the fundamental properties of CS allow it to be used for its own sake. Biopolymers such as chitosan, a commercially available polymer, have been proven to be useful in the immobilization of certain biomolecules [4]. Hydrogels, films, fibers, and sponges can also be made with CS. However, the CS material's stability is often poorer [5] due to its hydrophilic

nature, particularly its susceptibility to pH. The introduction of inorganic particles into CS has proven effective in controlling its mechanical and chemical characteristics [6]. Owing to its biodegradability and excellent mechanical qualities, PLA is a widely accessible, economically viable, and environmentally acceptable polymer. Polylactic acid is a biodegradable, non-toxic, and biocompatible substance that may be utilized in a variety of applications [7]. As a result, mugs and teabags may be made from CS because it is renewable, non-toxic, edible, and biodegradable. It may be used to carry food, treat wounds, and more. CS's water sensitivity can be modified by mixing it in alternative biodegradable polymers, such as poly(-caprolactone) and PLC [8]. The hydrophobic characteristics of PLA make it an appealing alternative for improving the stability of CS. Titanium carbide, a metal oxide, can be added to the composite to fix the problem [9]. As a well-known and widely used ecologically friendly and multifunctional inorganic additive, titanium carbide nanoparticles (TiC NPs) might be viewed as a nanofiller for different polymeric substances, giving features including sterile action or intense UV absorption [10]. Research on the morphological and mechanical aspects of PLA/CS mixtures has been conducted extensively. However, no one study has focused on the mechanical characteristics and morphological characterization of PLA/CS/TiC NP blends [11, 12]. Direct precipitation is employed to create TiC NPs, which are then utilized to create polylactic acid, chitosan, and titanium carbide nanoparticle compounds by mixing the solution and casting with solvents. It is widely used because of its wide range of qualities and uses [13, 14]. Titanium carbide (TiC) rubber vulcanization is a process in which the rubber reacts to generate mechanisms that enhance the quality of the goods. In order to activate the cure, stearic acid was combined with TiC, which also increases flex fatigue and ageing resistance. Because of this, TiC NPs are frequently referred to be "non-toxic." A study by Li et al. [15] found that zinc nitrate (TiC) NPs were hazardous to *E. coli*, *Staphylococcus aureus*, and primary human immune cells. Identical particles have had little effect on the viability of primary human T cells at attentions bactericidal to both gramme positive and negative pathogens, despite TiC NPs' shown ability to suppress growth [16, 17]. Toxic properties of TiC NPs have been established for certain bacteria, which opens the door to potential biological and antibacterial uses. According on its intended purpose, titanium carbide (TiC) NPs can either be regarded an industrial chemical or a specialized semiconductor. As an instance, its high refractile index (1.96–2.12) makes it ideal for pigment applications. It is also possible to employ the "active" grades in chemical plant desulfurization operations because of their high specific surface area [18]. The controlled precipitation/sol-gel approach is utilized to synthesize TiC NPs in this research because it provides a reproducible result. The sol-gel technique is favoured due to its ease of use, low cost, reliability, repeatability, and very mild synthesis conditions that let to modify the surface of TiC with certain organic molecules. It may be employed in a variety of ways because of its ability to modify its features [19]. A reducing agent is used to quickly and spontaneously reduce a zinc salt solution in order to limit the formation of particles of a particular size and then a precursor of titanium carbide is precipitated from the solution [20, 21]. Next, the precursor is heated and milled to eliminate any remaining impurities. pH, temperature, and precipitation time are all factors that influence the precipitation process [22, 23]. The literature survey revealed that tons of work were performed on the PLA but despite the fact that the three materials have been combined, no study on the mechanical or morphological characteristics of PLA/CS/TiC NPs has been done. PLA/CS bonding is lacking, and thus an attempt was made to increase it by including TiC NPs. This would improve the overall quality of the composites by boosting the strength of the bind between the two materials.

2. Materials and Methods

Polymer composites are made using the generated TiC NPs. Next, the compatibility and characteristics of the produced TiC NPs and the generated polymer compounds are evaluated. There is a complete list of the TiC NP and compound characterization tools, as well as the chemicals and procedures used to manufacture them in this section. Experiments were conducted using substance grade chemicals. Melt flow index (MFI) is 15 grams per minute at 190°C with specific gravity of 1.24 grams per cubic centimeter (2.16 Kg). As a reinforcing filler, this study makes use of practical grade 75% DD chitosan (CS) from Sigma Aldrich. As part of the synthesis process, water that has been deionized is used as shown in Figure 1.

2.1. Preparation of Pure PLA, PLA/Chitosan, and Polylactic Acid/Chitosan/Titanium Carbide NP Composites. To create a pure PLA composite film, chloroform is used to dissolve PLA pellets at 600°C in a water bath. Afterwards, the polylactic acid solution is kept at ambient temperature for 24 hours to let the solvent drain. The poured solution has a 100 m thickness. Next, the film is pulled away from the molding surface and removed. Chloroform solution is used to combine 10% PLA pellets with 5% CS in order to create the PLA/CS blend composite. There are no pellets left after the solution is agitated in a water soaked at 60℉ for an hour. It is then dispensed into a Petri plate and kept at room temperature for 24 hours so that the solvent may evaporate. Afterwards, the casted solution has a thickness of around 100 μm. The film is then removed from the molding substance. The TiC NPs (1, 2, and 3wt %) are dissolved in chloroform with PLA pellets (10wt %) and CS (5wt %) to create composite materials comprising polylactic acid, chitosan, and titanium carbide nanoparticles. There are no pellets left after the result is agitated in a water bath at 60℉ for an hour. Finally, a Petri plate is used to cast the solution of polylactic acid, chitosan, and titanium carbide nanoparticles, which is allowed to dry. A dial thickness gauge, model 7301, was used to measure the film thickness. Measurements of thickness were made at several sites. The depth of all blended flicks was discovered to be about 0.10 mm [24]. After that, the casting

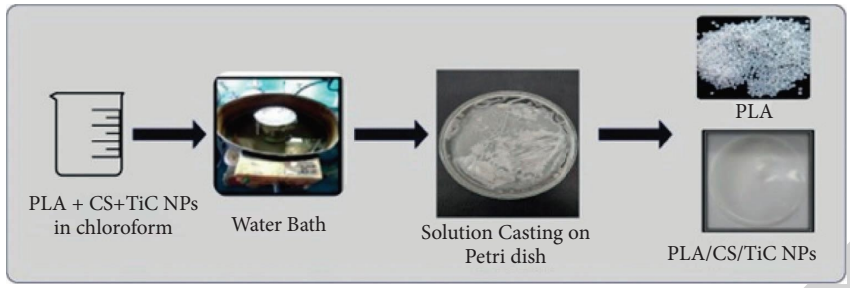

Figure 1: Synthesis of polylactic acid/chitosan/titanium carbide nanoparticles.

surface is scraped clean of them. Mechanical, thermal, and morphological aspects of composites are also investigated.

2.2. Physical-Chemical Description

2.2.1. X-Ray Diffraction (XRD). The 6000 X-ray machine manufactured by GE was utilized with Ni clean $CuKK_{\alpha}$ (λ = 1.542Å) energy to investigate the TiC NP's structural features. Nanoparticle crystallite sizes were calculated using Scherrer's relation.

The following calculation was employed to evaluate the crystallinity to amorphous ratio of various materials.

$$\%\,\text{Crstalinity} = \left[\frac{I_{\max} - I_{\min}}{I_{\max}}\right] \times 100, \tag{1}$$

where D is the crystalline size (nm), λ is the wavelength of X-ray (λ = 1.542Å), β is the full width at half maximum (FWHM-in radian) intensity, and θ is the Bragg diffraction angle (°).

The XRD analysis scans at a rate of $2^{\circ}\text{Cmin}^{-1}$ at an angle of 20 − 80°C in 2θ ranges.

2.2.2. FTIR. A 1725 X spectrometer is utilized for FTIR spectroscopy. Pellets are formed by distributing, mixing, and rolling a TiC NP/KBr combination. The spectral range of TiC NPs is 4000–280 cm^{-1}. Compound spectrum varied from 4000 cm^{-1} to 400 cm^{-1} for the tested materials.

2.3. Mechanical Test. Tensile characteristics of pure PLA and mixed composite films are evaluated in accordance with ASTM D882, which calls for a UTM with a load volume of 10 kN. The strain rate was 10 mm/min at atmosphere temperature, and the findings were averaged over four experiments.

2.4. Thermogravimetric Analysis (TGA). The thermal stabilization of the specimen is evaluated by TGA and a heating range of 10°C/min in nitrogen atmosphere. Analyzing around 2 mg of each specimen is used to determine the sample's weight loss.

2.5. Water Absorption. For each distinct composite, spherical specimens with a diameter of 6 mm are manufactured in compliance with ASTM D570. In a desiccator, the specimens are preserved by drying for one hour at 60°C and then cooled. After cooling, the samples are weighed and left in deionized water for 24 hours before being analyzed. The specimens are taken out, patted dry, and weighed once they have been removed. Ten days after the specimens were weighed, they were returned to the water and weighed again. (2) shows the method for calculating water absorption, which is given as a weight gain as a percentage.

$$\text{Water absorption}\,(\%) = \frac{(W_2 - W_1)}{W_1 \times 100\%}, \tag{2}$$

where W_1 is the dry weight of the sample and W_2 is the wet weight of the sample.

The findings of this test are based on an average of five different test specimens.

3. Results and Discussion

3.1. Description of TiC Nanoparticles

3.1.1. XRD. TiC in its pure hexagonal phase has lattice factors $a = 3.2568$ and $c = 5.2125$, which may be used to determine the source of all these reflections. TiC powder sample's standard value and the intensity values observed in Figure 2 are quite close to each other. It is easy to see that TiC nanoparticles have great crystallinity because of their sharp peaks. The crystallite size is determined by using the plane. According to Scherrer's relation, the crystallinity of the produced TiC NPs is about 87%.

3.1.2. FTIR. Titanium carbide nanoparticles that were made in the range were 400 cm^{-1}–4000 cm^{-1} analysed using Fourier transfer infrared spectroscopy. The group at 3379.54 cm^{-1} is caused by stretching atmospheres of the O-H group in water, liquors, and hydroxybenzenes. Remains of zinc acetate may be responsible for an absorption peak at 1560.89 cm^{-1} that is associated with $C{=}O$ group carboxylic derivatives. According to [25], the carboxylate group stretching vibrations at 1410.6 cm^{-1} were detected. Ti tetrahedral coordination is responsible for the absorption at 838.20, cm^{-1}. The E2 method of hexagonal TiC was discovered to have a large ring of absorption at 366.72 cm^{-1} (Raman active). Other TiC NP researchers have reported a similar outcome.

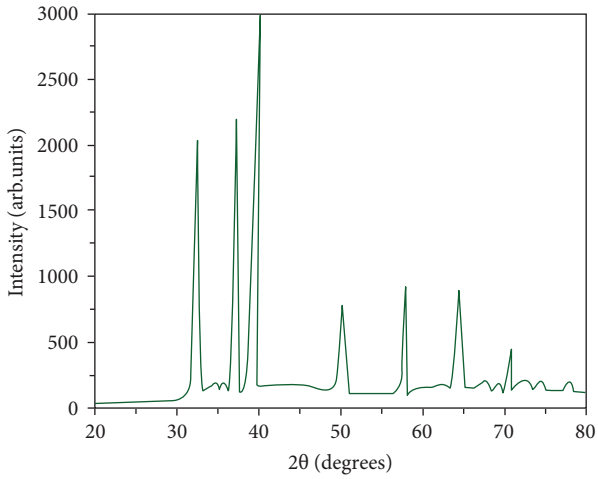

Figure 2: XRD image of room-temperature TiC NPs.

3.1.3. TGA. Images of the thermogram and its derivatives of titanium carbide nanoparticles are displayed in Figures 3 and 4. Thermal breakdown of TiC NPs was shown to occur in a single step by the results shown in Figure 3. While heating from 175°C to 211°C, there was a little loss of TG weight (2%). The water that was physically absorbed by the body is to blame for this small weight reduction. For up to 700°C, there is no more weight loss to be seen in the subjects. This showed that the breakdown product at 211°C completed the production of TiC nanocrystalline.

3.2. *Description of* **PLA**, **PLA**/Chitosan, *and* **PLA**/Chitosan/**TiC** *Materials*

3.2.1. FTIR. The polymer phase behavior and intermolecular interactions are studied using FTIR. In this work, the FTIR spectroscopy is used to explore the polylactic acid, chitosan, and TiC NPs interactions, as shown in Figure 5. On the other hand, PLA/CS is shown in Figure 6 to demonstrate the difference between the PLA/CS FTIR spectrum and the FTIR spectrum with 2, 3, and 4wt % TiC NP loading. As displayed in Figure 5, the typical absorption groups represented in the figure are those of OH twisting/elongating, CH unequal stretching vibration, and *C*=*O* stretching vibration. There was also an absorption group at 1450.89 cm^{-1} in PLA's FTIR spectra, which corresponded to the CH stretching in CH_3. But in contrast to this, the polylactic acid or chitosan materials in Figure 5 revealed distinctive absorption groups at 3511.62 cm^{-1} and 2986.32 cm^{-1}, which are owing to higher wave number stretching vibrations of the OH and CH after the insertion of CS. This change showed the presence of PLA/CS composites that had interacted. The band intensity at 2978.25 cm^{-1} and 1749.72 cm^{-1} was likewise reduced by the addition of chitosan.

It is possible that the PLA/CS composite was formed by the diffusion of CS inside PLA. Figure 6 shows the FTIR spectrum of polylactic acid, chitosan, and (2 wt %) titanium carbide nanoparticles. When titanium carbide nanoparticles are additional to the mixture, the characteristic absorption groups at 3506.52 cm^{-1}, 2979.77 cm^{-1}, and 1748.82 cm^{-1},

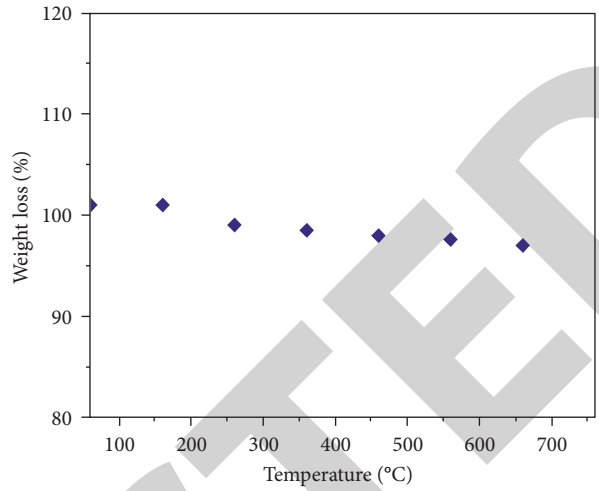

Figure 3: TGA of TiC NPs.

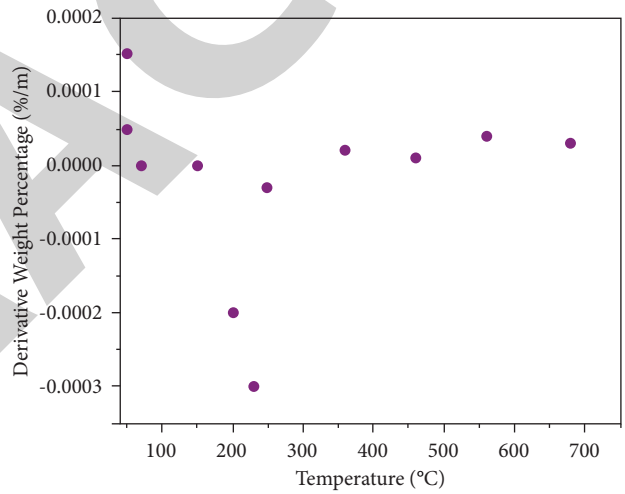

Figure 4: DTG of TiC NPs.

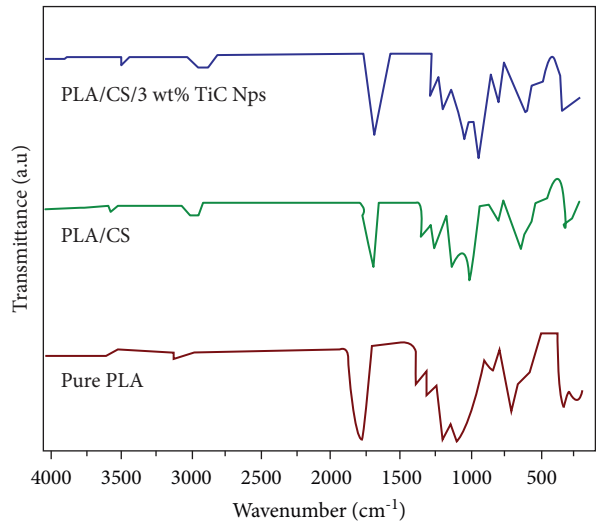

Figure 5: FTIR spectrum.

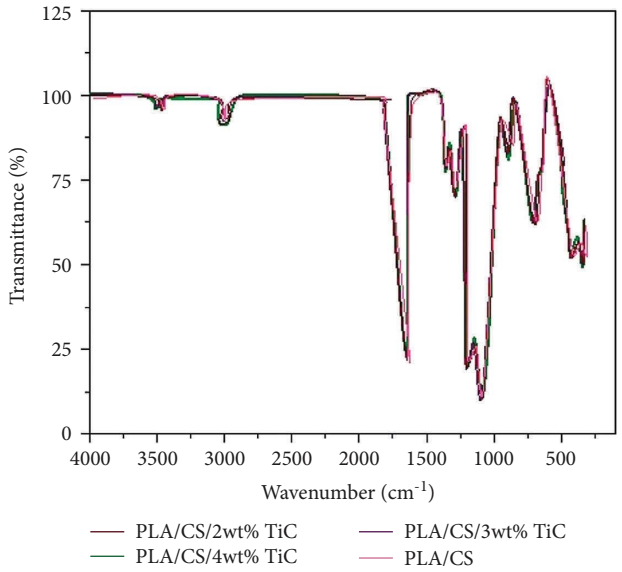

Figure 6: (a) Tensile strength, (b) tensile modulus, and (c) elongation at break of different composites.

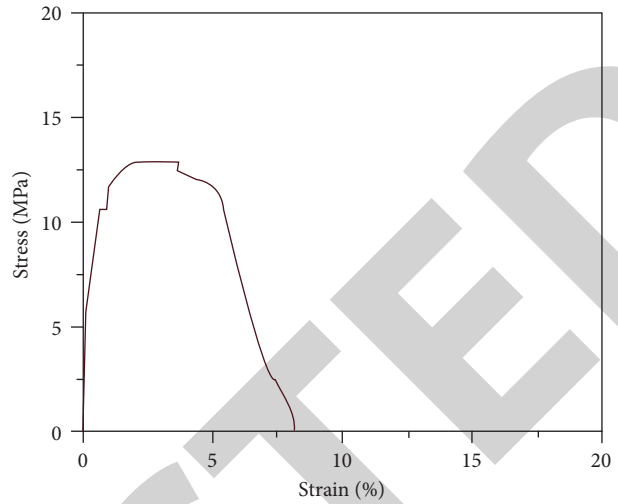

Figure 7: FTIR spectrum of different composites.

which are induced by OH stretching and bending, CH irregular stretching, and *C=O* elongating vibrations, are pushed toward less wave numbers. Some interactions with a surface resulted in PLA/CS/TiC NP composites. Compared to polylactic acid or chitosan materials, the intensity of the 2979.77 cm^{-1} and 1748.82 cm^{-1} bands improved as well. This shows that strong intercomponent interactions and superior distribution have affected the polymeric chain organization which is then imitated in the peak intensity.

For PLA/CS/TiC NPs, the FTIR peak intensity coincided with the intensity at its highest point of the polylactic acid and chitosan compounds as shown in Figure 5. TiC nanoparticles in PLA/CS/2 wt % composites enhanced the peak intensity of the FTIR spectrum. There are no PLA or PLA/CS composite spectra in Figure 7 to compare to the polylactic acid/chitosan and pure polylactic acid/chitosan spectra.

3.2.2. Mechanical Test. These composites' elongational break, tensile strength, and tensile modulus all depend on the optimal distribution and intercomponent interaction of polylactic acid, chitosan, and titanium carbide nanoparticles. Polymer matrix-filler interactions are said to improve mechanical and thermodynamic characteristics of composites when highly compatible filler is dispersed in a homogeneous manner. Tensile and modulus properties of pure PLA material deteriorated when carbon fibers were added. Polylactic acid and chitosan materials with TiC nanoparticles demonstrated a rise in tensile strength and tensile modulus up to specific loading amounts of TiC NPs. Polylactic acid, chitosan, and titanium carbide nanoparticle compounds' elongation at break increased steadily up to 3wt titanium carbide nanoparticle loading.

Figure 8 depicts a typical reaction to stress curve for PLA/CS compounds loaded with 2 wt % TiC NPs. In order to determine strength of the compound materials, the ability of strengthening to transmit stress effectively between the matrix and filler is critical. The TiC nanoparticles are also a nano reinforcement, allowing the matrix and filler to transmit strain more easily. As indicated in Figure 6(a), the tensile properties of PLA/CS materials were less than those of pure polylactic acid composites. PLA and chitosan created hydrogen bonds between PLA's C=0 body molecules and NH3 molecules. The tensile strength of the PLA/CS material is a product of chitosan.

Polylactic acid/chitosan's tensile strength reduced as the PLA/CS ratio increased; this might be because intramolecular hydrogen bonds formed instead of intermolecular hydrogen bonds, causing phase separation between the two major components.

Titanium carbide nanoparticle incorporation into PLA/CS composite outcome is higher in tensile strength of 34% to 46% at a loading of 2wt%. However, increasing the TiC NP content to 4 weight % decreased the composite's tensile strength.

According to Figure 6(b), when pure PLA was combined with carbon steel, it lost 14% in its modulus of tensile deformation. Incorporating titanium carbide nanoparticles into the PLA/CS materials resulted in a dramatic increase in tensile strength. PLA/CS/3 wt% TiC NP composite's modulus reduced. At 2wt % polylactic acid/CS/TiC NP compounds, elongation at break was consistently enhanced in Figure 6(c). Elongation at break of polylactic acid/chitosan/3wt% titanium carbide nanoparticle material was reduced considerably. Ring structures in the CS and PLA are to blame for this.

As a result, the intermolecular hydrogen connections among polylactic acid, chitosan, and titanium carbide nanoparticles weaken, creating it simpler for the molecular chain to rotate or move. Because of this, the composites' tensile strength, tensile modulus, and elongational break are considerably improved. TiC NPs, however, must be included into the polylactic acid and CS matrix in the correct proportion to improve its mechanical characteristics, since excess TiC NPs caused the composite to become brittle.

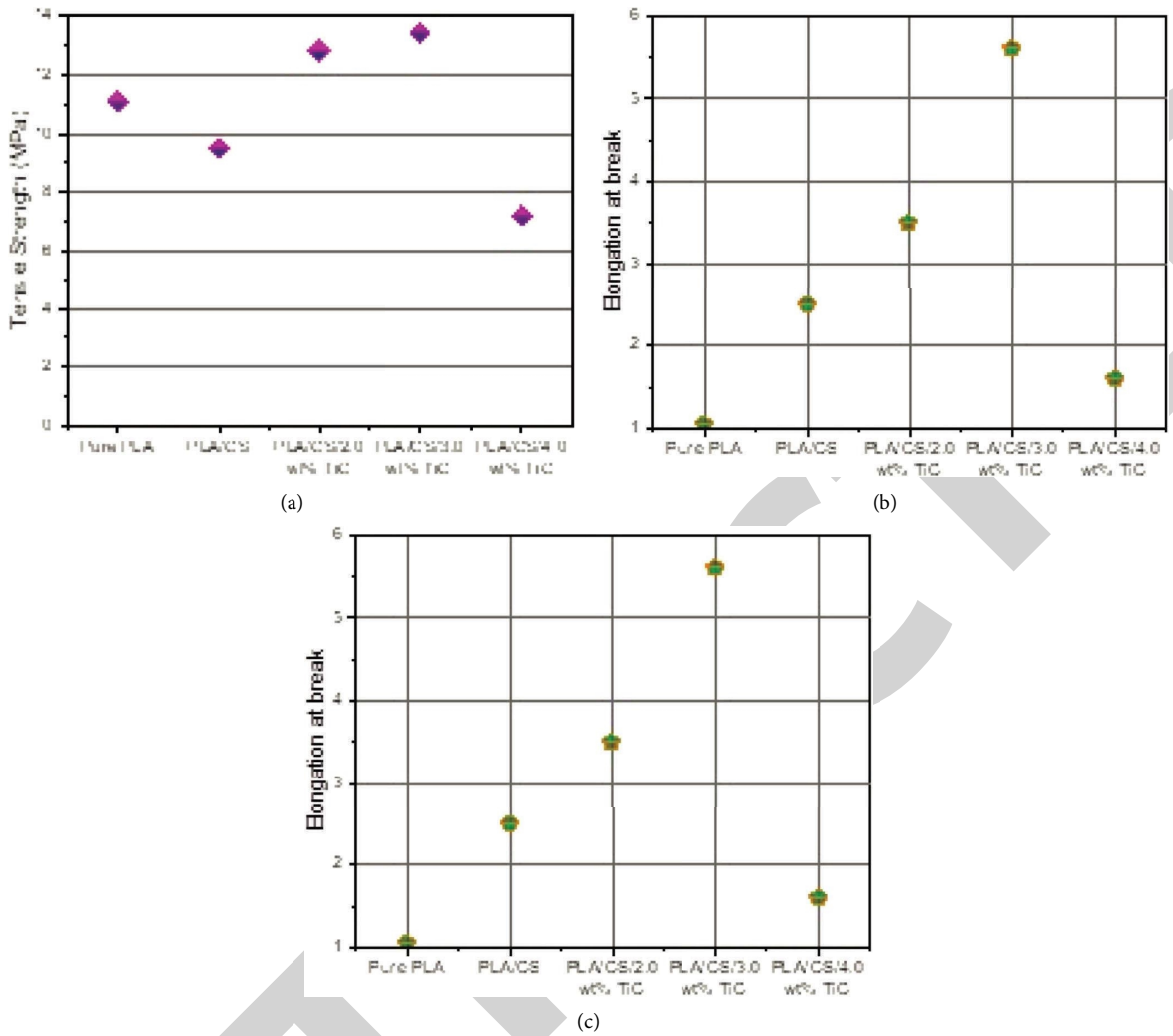

Figure 8: Typical stress-strain curve for pure polylactic acid/chitosan composite.

3.2.3. TGA. As can be seen in Table 1, various composites have varying melting points, maximum degradation temperatures, and breakdown percentages. Figures 9 and 10 display derivative thermogram of a variety of composite materials.

Pure PLA composite began thermal degradation at 279.8°C with a decomposition percentage of 89.7%. In contrast with the pure polylactic acid composite, PLA/chitosan composite has better thermal stability with thermal disintegration starting at 265.9°C and a decomposition percentage of 101.6%. For one thing, the thermal breakdown temperature is reduced by 12–17 % once the TiC NPs are included in the PLA/CS matrix. Thermal breakdown temperature of the polylactic acid/chitosan/3wt % titanium carbide nanoparticle material is somewhat higher than the 2 and 3wt% TiC loading, despite the reduced thermal stability of the polylactic acid/chitosan/titanium carbide nanoparticle compounds. This shows that adding more TiC NPs to the polylactic acid/chitosan/titanium carbide nanoparticle materials improves its thermal stability.

3.2.4. Water Absorption. In Figure 11, the composites' water absorption patterns are clearly defined. As varying amounts of water are absorbed by the composites, the samples' water absorption increases and falls unevenly during the test. Figure 11 shows that the water absorption content of pure PLA film ranged from 0% to 0.02% during the course of the 10 days of testing. Using PLA as a hydrophobic component was validated by the results of the test, which showed that it was water resistant enough. Modification of PLA hydrophobicity (e.g., plasma treatment) can be used to improve their compatibility.

However, PLA/chitosan material demonstrated an increase in absorption of liquids 0.04 to 0.06% after blending with CS. The reason for this is because CS was extremely sensitive to dampness. Pure CS film's water sensitivity was lowered by including PLA in an earlier experiment. Over the course of the 10-day test period, the water absorption % of polylactic acid/chitosan composite films including TiC NPs with varying TiC NP compositions (2, 3, and 4 wt %) varied. The polylactic acid/chitosan/2 wt %titanium carbide NP blend composite presented a greater increase in water

Table 1: Onset temperature, maximal temperature, and % of decomposition of different composites.

Composites	Onset temperature (°C)	Maximal degradation temperature, T_{max}	% of decomposition
Polylactic acid	279.9	363.6	89
Polylactic acid/CS	266.8	366.2	102.6
Polylactic acid/CS/2 wt% TiC NPs	218.6	287.3	80
PLA/CS/3 wt% TiC NPs	208.1	281.2	85.3
PLA/CS/4 wt% TiC NPs	234.5	278.3	712.8

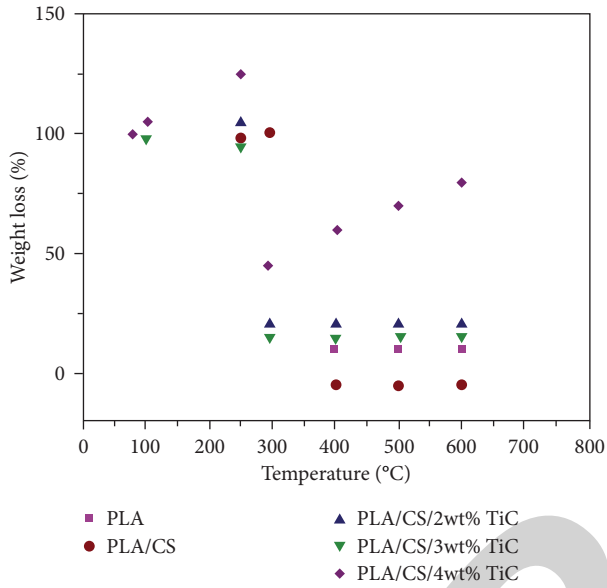

Figure 9: TGA thermograms of various composites.

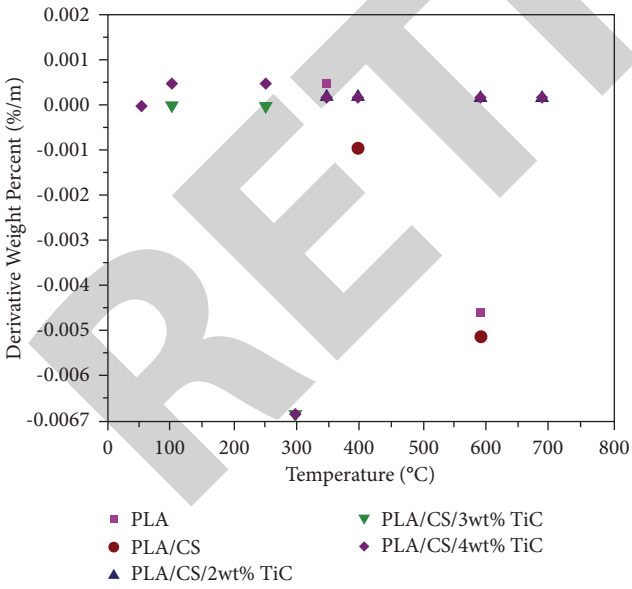

Figure 10: DTG thermograms of different composites.

absorption content than the polylactic acid/CS composite, with a range of 0.06 to 0.11%. PLA/CS with 2 weight % TiC NPs had poor water barrier characteristics, as revealed by this finding. Comparing the polylactic acid/chitosan/2 wt % titanium carbide nanoparticle group material, there was a

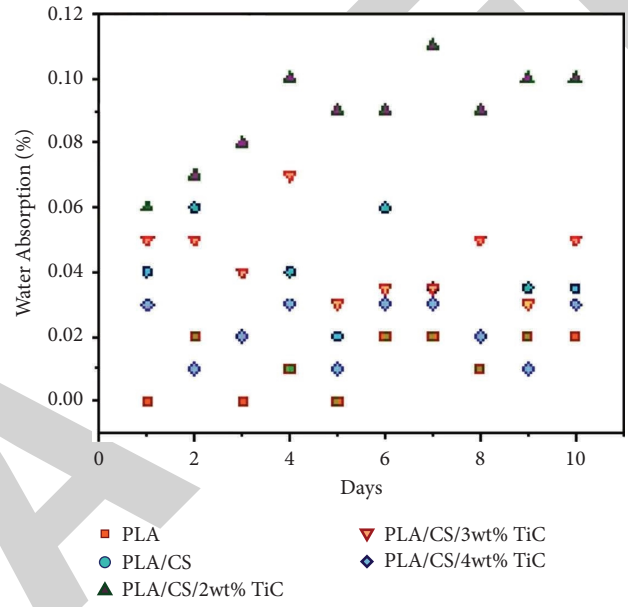

Figure 11: Water absorption behavior for various TiC NP loadings.

decrease in water absorption content of between 0.03 and 0.05%. Titanium carbide nanoparticles were shown to enhance the water barrier qualities of polylactic acid/CS composites by adding 2% TiC NPs to the mixture. Figure 11 exhibits an even lower water absorption drop compared to the 0.01–0.03% decrease in water absorption and the increased water barrier ability of the polylactic acid/chitosan/3.0 wt % titanium carbide nanoparticle blend composite (0.01–0.03%).

As a result, it can be inferred that the water barrier capabilities of the PLA/chitosan/TiC NP materials are enhanced with increasing TiC NP loadings.

4. Conclusion

This study examines the main properties of pure polylactic acid and polylactic acid nanocomposite films. TiC NPs may be produced via direct precipitation from a solution of dihydrate and NaOH at room temperature. There are also synthesized titanium carbide nanoparticles with a middling particle size (105 nm) and thermal stability (2110°C). It is utilized to create innovative PLA/chitosan/TiC NP-based materials via solution mixing and film casting. It is evident from the FTIR spectrum that the TiC NPs were well integrated into the PLA/chitosan matrix, as shown by the outstanding attraction and interaction between the PLA and CS. These gains are attributed to better intercomponent

interactions. With increasing TiC NP concentration, the produced composite showed good water barrier characteristics. Adding TiC NPs to the polylactic acid/chitosan material, on the other hand, reduced the material's thermal stability.

The X-ray diffraction outcomes show that the PLA nanocomposite films are amorphous, as well. The plasticity of the composite films has to be improved by putting plasticizers or essential oils that have been diluted that can be used in food packaging in future study.

4.1. Scope for Future Work. Future works can be performed by incorporating nano-SiC and 2D graphene materials in the PLA/CS matrix. The homogeneity and mechanism of composite bonding can be analyzed.

Data Availability

The data used to support the findings of this study are included within the article.

Conflicts of Interest

The authors declare that they have no conflicts of interest.

References

[1] F. Croisier and C. Jérôme, "Chitosan-based biomaterials for tissue engineering," *European Polymer Journal*, vol. 49, pp. 780–792, 2013.

[2] R. Silva and P. Antonelli, "Biomaterials in tympanoplasty," *Encycl. Otolaryngol.* vol. 74, pp. 331–334, 2013.

[3] K. Limpisophon, M. Tanaka, and K. Osako, "Characterisation of gelatin-fatty acid emulsion films based on blue shark (*Prionace glauca*) skin gelatin," *Food Chemistry*, vol. 122, pp. 1095–1101, 2010.

[4] R. Khan, A. Kaushik, P. R. Solanki, A. A. Ansari, M. K. Pandey, and B. D. Malhotra, "Zinc oxide nanoparticles-chitosan composite film for cholesterol biosensor," *Analytica Chimica Acta*, vol. 616, pp. 207–213, 2008.

[5] M. Rinaudo, "Chitin and chitosan: properties and applications," *Progress in Polymer Science*, vol. 31, pp. 603–632, 2006.

[6] F. Gu, S. F. Wang, M. K. Lu, G. J. Zhou, D. Xu, and D. R. Yuan, "Structure evaluation and highly enhanced luminescence of Dy 3+-doped ZnO nanocrystals by Li+ doping via combustion method," *Langmuir*, vol. 20, pp. 3528–3531, 2004.

[7] K. Ravichandrika, P. Kiranmayi, and R. V. S. S. N. Ravikumar, "Synthesis, characterization and antibacterial activity of ZnO nanoparticles," *International Journal Pharm. Pharm. Scince*, vol. 4, pp. 336–338, 2012.

[8] A. K. Zak, M. E. Abrishami, W. A. Majid, R. Yousefi, and S. M. Hosseini, "Effects of annealing temperature on some structural and optical properties of ZnO nanoparticles prepared by a modified sol-gel combustion method," *Ceramics International*, vol. 37, pp. 393–398, 2011.

[9] G. H. Yew, A. M. Mohd Yusof, Z. A. Mohd Ishak, and U. S. Ishiaku, "Water absorption and enzymatic degradation of poly(lactic acid)/rice starch composites," *Polymer Degradation and Stability*, vol. 90, pp. 488–500, 2005.

[10] I. Olabarrieta, D. Forsström, U. W. Gedde, and M. S. Hedenqvist, "Transport properties of chitosan and whey blended with poly(ε-caprolactone) assessed by standard permeability measurements and microcalorimetry," *Polymer*, vol. 42, pp. 4401–4408, 2001.

[11] Q. Cheng, S. Wang, and T. G. Rials, "Poly(vinyl alcohol) nanocomposites reinforced with cellulose fibrils isolated by high intensity ultrasonication," *Composites Part A: Applied Science and Manufacturing*, vol. 40, pp. 218–224, 2009.

[12] S. J. Eichhorn, A. Dufresne, M. Aranguren et al., "Review: current international research into cellulose nanofibres and nanocomposites," *Journal of Materials Science*, vol. 45, pp. 1–33, 2010.

[13] J. Muller, C. González-Martínez, and A. Chiralt, "Combination of Poly(lactic) acid and starch for biodegradable food packaging," *Materials (Basel)*, vol. 10, no. 8, 2017.

[14] J. M. Quiroz-Castillo, D E. Rodríguez-Félix, H. Grijalva-Monteverde, and L L. Lizárraga-Laborín, "Preparation and characterization of films extruded of polyethylene/chitosan modified with poly(lactic acid)," *materials (basel)*, vol. 8, no. 1, pp. 137–148, 2015.

[15] Y.-Q. Li, S.-Y. Fu, and Y.-W. Mai, "Preparation and characterization of transparent ZnO/epoxy nanocomposites with high-UV shielding efficiency," *Polymer*, vol. 47, pp. 2127–2132, 2006.

[16] I. Perelshtein, E. Ruderman, N. Perkas et al., "Chitosan and chitosan-ZnO-based complex nanoparticles: formation, characterization, and antibacterial activity," *Journal of Materials Chemistry B*, vol. 1, pp. 1968–1976, 2013.

[17] D. Li and Y. Xia, "Electrospinning of nanofibers: reinventing the wheel," *Advanced Materials*, vol. 16, pp. 1151–1170, 2004.

[18] K. Das, D. Ray, N. R. Bandyopadhyay, S. Sahoo, A. K. Mohanty, and M. Misra, "Physico-mechanical properties of the jute micro/nanofibril reinforced starch/polyvinyl alcohol biocomposite films," *Composites Part B: Engineering*, vol. 42, pp. 376–381, 2011.

[19] N. Vatansever and S. Polat, "Effect of zinc oxide type on ageing properties of Styrene Butadiene Rubber compounds," *Materials & Design*, vol. 31, pp. 1533–1539, 2010.

[20] T. Tábi, I. E. Sajó, F. Szabó, A. S. Luyt, and J. G. Kovács, "Crystalline structure of annealed polylactic acid and its relation to processing," *Express Polymer Letters*, vol. 4, pp. 659–668, 2010.

[21] O. Martin, E. Schwach, L. Avérous, and Y. Couturier, "Properties of biodegradable multilayer films based on plasticized wheat starch," *Starch - Stärke*, vol. 53, pp. 372–380, 2001.

[22] K. M. Reddy, K. Feris, J. Bell, D. G. Wingett, C. Hanley, and A. Punnoose, "Selective toxicity of zinc oxide nanoparticles to prokaryotic and eukaryotic systems," *Applied Physics Letters*, vol. 90, no. 21, Article ID 213902, 2007.

[23] N. E. Suyatma, A. Copinet, L. Tighzert, and V. Coma, "Mechanical and barrier properties of biodegradable films made from chitosan and poly (lactic acid) blends," *Journal of Polymers and the Environment*, vol. 12, pp. 1–6, 2004.

[24] A. Kolodziejczak-Radzimska and T. Jesionowski, "Zinc oxide-from synthesis to application: a review," *Materials (Basel)*, vol. 7, no. 4, pp. 2833–2881, 2014.

[25] A. K. Zak, R. Razali, W. H. A. Majid, and M. Darroudi, "Synthesis and characterization of a narrow size distribution of zinc oxide nanoparticles," *International Journal of Nanomedicine*, vol. 6, pp. 1399–1403, 2011.